


## RESOURCE ARTICLE

A chromosome-level genome assembly of *Pyropia haitanensis* (Bangiales, Rhodophyta)

Min Cao<sup>1,2</sup>  | Kuipeng Xu<sup>1,2</sup> | Xinzi Yu<sup>1,2</sup> | Guiqi Bi<sup>1,2</sup> | Yang Liu<sup>1,2</sup> | Fanna Kong<sup>1,2</sup> |  
Peipei Sun<sup>1,2</sup> | Xianghai Tang<sup>1,2</sup> | Guoying Du<sup>1,2</sup> | Yuan Ge<sup>1,2</sup> | Dongmei Wang<sup>1,2</sup> |  
Yunxiang Mao<sup>1,2,3,4</sup>

<sup>1</sup>Key Laboratory of Marine Genetics and Breeding (OUC), Ministry of Education, Qingdao, China

<sup>2</sup>College of Marine Life Sciences, Ocean University of China, Qingdao, China

<sup>3</sup>Laboratory for Marine Biology and Biotechnology, Qingdao National Laboratory for Marine Science and Technology, Qingdao, China

<sup>4</sup>Key Laboratory of Utilization and Conservation for Tropical Marine Bioresources (Hainan Tropical Ocean University), Ministry of Education, Sanya, China

## Correspondence

Yunxiang Mao and Dongmei Wang, Key Laboratory of Marine Genetics and Breeding (OUC), Ministry of Education, Qingdao, China.

Emails: yxmao@ouc.edu.cn; wangdm@ouc.edu.cn

## Funding information

This work was financially supported by the National Key R&D Program of China (2018YFD0900106), the Marine S&T Fund of Shandong Province for Pilot National Laboratory for Marine Science and Technology (Qingdao) (No. 2018SDKJ0302-5), the Fundamental Research Funds for the Central Universities (201762016) and the Project of National Infrastructure of Fishery Germplasm Resources (2018DKA30470). These funding bodies had no role in the study design, analysis, decision to publish or preparation of the manuscript.

## Abstract

*Pyropia haitanensis* (Bangiales, Rhodophyta), a major economically important marine crop, is also considered as an ideal research model of Rhodophyta to address several major biological questions such as sexual reproduction and adaptation to intertidal abiotic stresses. However, comparative genomic analysis to decipher the underlying molecular mechanisms is hindered by the lack of high-quality genome information. Therefore, we integrated sequencing data from Illumina short-read sequencing, PacBio single-molecule sequencing and BioNano optical genome mapping. The assembled genome was approximately 53.3 Mb with an average GC% of 67.9%. The contig N50 and scaffold N50 were 510.3 kb and 5.8 Mb, respectively. Additionally, 10 superscaffolds representing 80.9% of the total assembly (42.7 Mb) were anchored and orientated to the 5 linkage groups based on markers and genetic distance; this outcome is consistent with the karyotype of five chromosomes ( $n = 5$ ) based on cytological observation in *P. haitanensis*. Approximately 9.6% and 14.6% of the genomic region were interspersed repeat and tandem repeat elements, respectively. Based on full-length transcriptome data generated by PacBio, 10,903 protein-coding genes were identified. The construction of a genome-wide phylogenetic tree demonstrated that the divergence time of *P. haitanensis* and *Porphyra umbilicalis* was ~204.4 Ma. Interspecies comparison revealed that 493 gene families were expanded and that 449 were contracted in the *P. haitanensis* genome compared with those in the *Po. umbilicalis* genome. The genome identified is of great value for further research on the genome evolution of red algae and genetic adaptation to intertidal stresses.

## KEYWORDS

comparative genomic analysis, genome annotation, genome assembly, *Pyropia haitanensis*, repeat annotation, whole-genome sequencing

Min Cao, Kuipeng Xu, Xinzi Yu, Guiqi Bi contributed equally to this work.

This is an open access article under the terms of the Creative Commons Attribution NonCommercial License, which permits use, distribution and reproduction in any medium, provided the original work is properly cited and is not used for commercial purposes.

© 2019 The Authors. Molecular Ecology Resources published by John Wiley & Sons Ltd

## 1 | INTRODUCTION

Red algae (Rhodophyta) are an ancient eukaryotic group that extended back to 1.6–1.0 billion years ago according to the observation of the cellular and subcellular structures of multicellular rhodophytes *Rafatazamia* and *Ramathallus* in fossils using synchrotron radiation X-ray tomographic microscopy (Bengtson, Sallstedt, Belivanova, & Whitehouse, 2017). Red algae comprise a monophyletic lineage of ~7,200 photosynthetic species, which belong to the Archaeplastida (Plantae) derived from primary endosymbiosis (Yoon, Müller, Sheath, Ott, & Bhattacharya, 2006). The secondary and tertiary endosymbiosis of red algae have given rise to the most abundant, species-rich and ecologically significant groups of algae and other eukaryotes present on Earth today, such as cryptophytes, haptophytes, apicomplexans, stramenopiles and dinoflagellates (Archibald, 2012; Hoek, Mann, Jahns, & Jahns, 1995; Reyes-Prieto, Weber, & Bhattacharya, 2007). Genomic studies on red algae will provide valuable information on the evolution of oxygenic photosynthesis. Unfortunately, only a limited number of whole-genome data sets for red algae have been reported, including those for the hot-spring alga *Cyanidioschyzon merolae*, the mesophilic alga *Porphyridium purpureum*, the extremophilic alga *Galdieria sulphuraria*, as well as the multicellular red seaweeds *Chondrus crispus*, *Gracilariopsis chorda* and *Porphyra umbilicalis* (Bhattacharya et al., 2013; Brawley et al., 2017; Collén et al., 2013; Lee et al., 2018; Nozaki et al., 2007). The genomic information of *Pyropia haitanensis* would help to reveal the adaptation mechanisms of intertidal seaweeds and help to reconstruct the evolutionary history of red algae.

In Rhodophyta, several species of the genus *Pyropia* (previously named *Porphyra*, and commonly called “*nori*”) are well known for their economic value in the seaweed industry, such as *P. haitanensis*, *P. yezoensis* and *P. tenera* (Sutherland et al., 2011). According to the FAO's statistics, nori production in the year 2016 was ~1.8 million tons in fresh weight with a commercial value over 1.5 billion USD (<http://www.fao.org/fishery/factsheets/en>). *Pyropia haitanensis* is a native species distributed along the coastline of south China. This species is cultivated at a large scale with the highest annual production among all the nori species. The current total annual harvest of *P. haitanensis* is ~88,000 tons (dry weight), which accounts for approximately 75% and more than 50% of the total nori production in China and the world, respectively (Guo et al., 2018). With the aid of a high-quality genome of *P. haitanensis*, modern molecular genetic techniques such as QTL mapping and GWAS will be used to identify the key loci of the important economic traits such as productivity, taste and colour, which undoubtedly will enhance the efficiency of molecular breeding of this economically important marine crop.

*Pyropia haitanensis* naturally inhabits a niche in the upper region of the intertidal zone (Sahoo, Tang, & Yarish, 2002). Routine tidal turning periodically exposes it to the air, and it inevitably experiences the drastic changes in environmental factors such as osmotic pressure, temperature, light and UV radiation (Blouin, Brodie, Grossman, Xu, & Brawley, 2011). *P. haitanensis* can survive even after losing 85%–95% of its cellular water (Wang, Mao, Kong, Cao, & Sun,

2015). The thriving nature of *P. haitanensis* suggested that long-term evolutionary selection has made this species highly adaptable to the combined harsh stresses of the intertidal region. Thereby, this species is considered a model of intertidal red seaweed for physiology and genetic research on stress tolerance. Due to its distinctive evolutionary position in the red algal clade, *P. haitanensis* might harbour different genetic mechanisms of stress tolerance from those of high plants, which are probably derived from green algae. The genome information of *P. haitanensis* is a valuable source for the identification of unique genetic signatures involved in environmental adaptation.

Furthermore, genome sequences of *P. haitanensis* with relatively higher integrity and completeness are unavailable, which has been one of the major constraints to improve research on the physiology, cytology, genetics and genomics of *Pyropia*. Currently, the development of high-throughput sequencing technologies for sequencing DNA, RNA and proteins has reduced sequencing time and cost, etc. Hitherto, there are already four generations. Every sequencing generation and its relevant sequencing platforms have advantages and disadvantages. Thus, it is necessary to assess their limitations and applications. Second-generation sequencing is currently the most common because of its higher throughput, but the short-read lengths and amplification biases have become disadvantages (Ari & Arikan, 2016). Single-molecule real-time (SMRT) is another sequencing technology that is currently in use, which can overcome the short-read lengths and biases without any amplification step (Roberts, Carneiro, & Schatz, 2013). The appearance of an optical map can further place short reads on genomic fragments, even those totalling several millions of bases (Neely, Deen, & Hofkens, 2011). Hence, in this study, the combined techniques of Illumina short-read sequencing, PacBio single-molecule sequencing and BioNano optical mapping were used to assemble the genome of *P. haitanensis*. Subsequently, gene prediction, repeat annotation, functional annotation, gene family expansion and contraction, and phylogenetic relationship were determined according to standard procedures to elucidate the gene repertoire of *P. haitanensis*.

## 2 | MATERIALS AND METHODS

### 2.1 | Sample information

A laboratory-cultured genetically pure line, *Pyropia haitanensis* PH40 (♀), was used in this study to eliminate the interference caused by genotypic differences. The original thallus was collected from a nori farm in Putian, Fujian Province, China. The material was first identified by amplification of its 18S rRNA gene as described in a previous study (Müller, Sheath, Vis, Crease, & Cole, 1998), as well as by its morphologies. Single somatic cells were enzymatically isolated from the thallus, and the allele homozygous sporophytes (conchocelis) were obtained after the haploid doubling spontaneously. The genetically homogenous gametophytes were then developed from the homozygous sporophytes and cultured for DNA and RNA sample collection. Another strain PH37 (♂) used in this study was also harvested from Putian, Fujian Province, China, and purified with

the same method mentioned above. The gametophytes were cultured in a light incubator under the following conditions:  $20 \pm 1^\circ\text{C}$  with  $50\text{--}60 \mu\text{mol photons}\cdot\text{m}^{-2}\cdot\text{s}^{-1}$  illumination during a 12 h:12 h light:dark cycle. The culture medium of Provasoli's enriched seawater (PES) (Starr, 1987) was refreshed every five days. To remove surface bacteria from *P. haitanensis* gametophytes, the thalli were harvested and mixed with quartz sands. Physical vibration was carried out in a homogenizer (Precellys 24), followed by several rounds of washing to remove the polysaccharides and bacteria from the surface of gametophytes. Subsequently, the samples were collected and immediately frozen in liquid nitrogen for total genomic DNA extraction using the CTAB method (Yang, Wang, Liu, & An, 1999).

## 2.2 | Libraries construction

Five micrograms and  $10 \mu\text{g}$  of genomic DNA were used to construct Illumina TruSeq paired-end sequencing libraries (500-bp insert sizes) and mate pair libraries (5 kb in size), respectively, according to the manufacturer's instructions. Meanwhile, a total of  $10 \mu\text{g}$  of DNA was used to construct a 20-kb library using the PacBio Pacific Biosciences SMRT Bell Template Kit 1.0. To further carry out optical map construction,  $2 \mu\text{g}$  of purified high molecular weight (HMW) genomic DNA was isolated and labelled according to standard BioNano protocols with the single-stranded nicking endonuclease BspQI. To assist in the genome annotation of *P. haitanensis*, total RNAs isolated from various stressful conditions (osmotic pressure, temperature, illumination, etc.) were equally mixed together to prepare the transcriptome sequencing libraries for SMRT platforms following the manufacturer's instructions. For SMRT sequencing, full-length RNA libraries were constructed according to the manufacturer's instructions with minor modifications. To avoid overamplification of small fragments, we optimized the amplification cycle at 14 in a preliminary test. Then, three gel fractions, containing fragments  $>3$ , 2–3 and 1–2 kb, were collected and purified using the QIAquick Gel Extraction Kit. The extracted products were amplified using the 5' Primer IIA and purified using  $0.5 \times$  AMPure beads (#A63880; Beckman, <http://www.beckmancoulter.com>) for subsequent sequencing.

## 2.3 | Genome sequencing and assembly

To estimate the genome size of *P. haitanensis*, the low-quality reads and sequences aligning to the chloroplast (Accession no: KC464603) and mitochondrion (NC\_017751) genomes of *P. haitanensis* were removed using the NGS QC Toolkit and Bowtie 2 (parameters: -very-sensitive; version: 2.0.2) (Langmead, Trapnell, Pop, & Salzberg, 2009). Different K-mer frequencies were calculated by Jellyfish and genome size (Luo et al., 2012). For genome assembly, subreads from PacBio were used to assemble the nuclear genome of *P. haitanensis* using the RS\_HGAP\_Assembly.3 protocol in SMRT ANALYSIS v2.3.0 with default parameters (Chin et al., 2013). Then, mate pair data sets were aligned to the above-assembled contigs using SSPACE (Boetzer, Henkel, Jansen, Butler, & Pirovano, 2010). Meanwhile, PacBio long

reads were mapped to the scaffold sequences using BLASR, and the gaps that resulted from the scaffolds were filled using PBJelly2 with default parameters (English et al., 2012). Finally, Quiver was run again to polish the accurate consensus at the base level.

To improve the assembly, optical maps of the BioNano system were further used for scaffolding. A labelled DNA sample was loaded onto the Saphyr Chip nanochannel array, and the stretched DNA molecules were then imaged with the BioNano Saphyr system. Raw image data were converted into bnx files, and AutoDetect (BioNano Genomics) software generated basic labelling and DNA length information. Access (BioNano Genomics) software was used to filter and remove  $<150$  Kb low-quality reads, and then, IrySolve (BioNano Genomics) was used to carry out the assembly of BioNano's genome maps and the 'Hybrid Scaffold' between genome maps from BioNano and sequence maps. Further gap filling using the reads that not used in the last step was achieved by RefAligner (BioNano Genomics). To remove the potential contamination of bacterial sequences in the current assembly, we applied a postprocessing step. We cut each scaffold into 100 bp overlapping 1-Kb windows and blasted them against the NT database using BLASTn. The blast results were further analysed using MEGAN to search for bacterial hits. Scaffolds that met the following three criteria were considered to be bacterial contamination and removed from the final genome: (a) over 60% of windows in the scaffold had best hits as bacterial sequences with identity  $>70\%$ ; (b) the sequencing depth was  $<5$ ; and (c) there was no cDNA support in these 'bacterial windows.' To assess the quality of the assembled genome, K-mer frequency distribution, the full-length transcriptome sequencing data map rate and Benchmarking Universal Single-Copy Orthologs (BUSCO) analysis were used.

## 2.4 | Genetic map construction and scaffold anchoring

To construct a genetic map of *P. haitanensis*, the gametophytic blades of PH40 ( $\varphi$ ) and PH37 ( $\delta$ ) were selected as parents for crossing experiments. The blades from these two pure lines were cocultured in a flask until carposporangia appeared. Then, the fertilized female blade was selected and cultured until reproductive cells were released. Subsequently, the fertilized carpospores were cultured to generate heterozygous conchocelis. The heterozygote was then confirmed using two SSR markers in our laboratory. After confirmation, the heterozygous gametophytes (F1) were then developed from the homozygous conchocelis and used to establish double haploid populations (DH). Each individual F1 gametophyte was digested into single cells using snail enzymes. Then, a single cell from each gametophyte was picked out and cultured to conchocelis. The cultured conditions were the same as those described above. Finally, a population with 117 DH strains was established and used for genetic map construction. Genomic DNA from two parents and 117 offspring were extracted using the CTAB method. DNA quality was detected with 0.8% agarose gel electrophoresis and a NanoDrop 2000 spectrophotometer. Then, 119 2b-RAD libraries were constructed according to the protocols described by Wang et al. (Wang,

Meyer, McKay, & Matz, 2012). These libraries were sequenced on an Illumina HiSeq system to generate single-end reads with a length of 50bp. Subsequently, reads were trimmed to remove sequences with adapters, those without restriction sites and those containing ambiguous bases and of low-quality value. Meanwhile, sequence reads from putative plastid and mitochondrial origins of *P. haitanensis* were also removed. The remaining reads were analysed using the RADtyping program v1.0 with default parameters (Fu et al., 2013) for genotyping. The markers that could be genotyped in at least 80% of offspring were used to calculate the genetic distance and draw linkage maps using JoinMap 4.0 at LOD 7.0 (Van Ooijen, 2006). The linkage group numbers were selected at a LOD threshold of more than 4.0. Meanwhile, genetic distances between markers and marker sequences were used to anchor scaffolds to the linkage groups using the R package.

## 2.5 | Repeat elements

Repeat elements occupy a major proportion of the nuclear DNA in most eukaryotic genomes and have been demonstrated to have structural and functional roles (Biscotti, Olmo, & Heslop-Harrison, 2015). REPEATMODELER (version: 1.0.8) was used to analyse consensus sequences of interspersed repeats in genomes of *P. haitanensis* (Smit & Hubley, 2008). Consensus sequences that were shorter than 80 bp were discarded (Wicker et al., 2007). The remaining consensus sequences were used as the library in REPEATMASKER (version: open-4-0-7) to predict interspersed repeat elements in the whole genome (Chen, 2004). Meanwhile, Tandem Repeats Finder (Benson, 1999) was used to identify tandem repeat sequences in *P. haitanensis* genome.

## 2.6 | Gene prediction and functional annotation

After repeats' masking, we used a combination of de novo prediction, homology searches and transcript isoform based methods to predict gene structures of *P. haitanensis*. De novo prediction was performed using AUGUSTUS (Stanke et al., 2006). For homologous annotation, we queried the *P. haitanensis* genome scaffolds against a database containing protein sequences from five organisms (*Chondrus crispus*, *Gracilariopsis chorda*, *Cyanidioschyzon merolae*, *Po. umbilicals* and *Porphyridium purpureum*). At the same time, transcript isoforms of *P. haitanensis* were mapped to the genome using BLAST and then assembled by PASA (Haas et al., 2008). Finally, EVM was used to integrate these gene models from the above methods. To further detect the function of the protein-coding genes in *P. haitanensis*, the predicted protein sequences were aligned against several public databases (NR, InterPro, GO, KOG, KEGG, CAZyme and Conserved Domains Database [CDD]).

## 2.7 | Gene family expansion and contraction

To further examine the genome divergence and conservation among red algae, we carried out a phylogenetic analysis based on single-copy

orthologous groups using the *P. haitanensis* genome and other five red algal genomes to build orthologous genes using ORTHOMCL (Li, Stoeckert, & Roos, 2003), with *Cyanophora paradoxa* as the out-group species. Genome sequences were aligned using the program MAFFT version 5 (Kato, Kuma, Toh, & Miyata, 2005) and were further trimmed using trimAl with the option "automated1" (Capella-Gutiérrez, Silla-Martínez, & Gabaldón, 2009). Maximum likelihood (ML) analyses were conducted using RAXML-8.2.4 (Stamatakis, 2014). The best model and parameter settings were chosen according to the Akaike information criterion using PROTTEST 3.0 (Abascal, Zardoya, and Posada 2005). A Bayesian phylogenetic tree was constructed using MRBAYES 3.2 under the same model (Huelsenbeck & Ronquist, 2001). Four incrementally heated Metropolis-coupled Monte Carlo Markov chains were run for 10,000,000 generations for the concatenated data set, and runs were sampled every 1000th generation. Convergence and stationarity of the log-likelihood and parameter values were assessed using TRACER v.1.5 (Rambaut, Drummond, Xie, Baele, & Suchard, 2018). The initial 10% were discarded as burn-in. A time-calibrated phylogeny was inferred using a relaxed molecular clock method as implemented in BEAST v.1.8.3 (Drummond, Suchard, Xie, & Rambaut, 2012). We set the most recent common ancestor with a lognormal prior, an offset of 950 Ma, and a standard deviation of 25.0 based on the divergence of Florideophyceae and Bangiophyceae (Herron, Hackett, Aylward, & Michod, 2009; Yang et al., 2016).

## 3 | RESULTS AND DISCUSSION

### 3.1 | Material identification and Genome assembly

The material used in this study was identified as *Pyropia haitanensis* according to its morphology, life history, as well as its reproductive structure, etc (Figure 1). The blade was 15–16 cm in length and 2–3 cm in width, with a red to brown colour. Additionally, it had an umbilicate base, which can help the blade attach to substratum. The molecular marker and alignment results also supported identification of the specimen as *P. haitanensis* (Figure S1). Scanning electron microscopy showed that bacteria had been removed from the surface of the algae (Figure S2). And a total of ~22.1 Gb of raw sequence data were obtained using the Illumina platform for *P. haitanensis*. Based on calculation of the K-mer frequency by Jellyfish, the estimated genome size of *P. haitanensis* was approximately 38.5 Mb (Table S1). For genome assembly, ~5.0 Gb of subreads from the PacBio RSII platform with a mean length of 5.7 kb were used to assemble the nuclear genome of *P. haitanensis*. A 59.7 Mb assembly was produced consisting of 1,839 contigs with an N50 of 510.3 kb. Then, the number of scaffolds built based on ~1.8 Gb of Illumina mate pair sequencing data was reduced to 1,168 and the length of N50 increased to 913.7 kb. Scaffolding using PacBio long reads allowed us to improve the assembly to 663 scaffolds (totalling 59.2 Mb) with a scaffold N50 of 912.3 kb. For optical map construction, a total of 93.8 Gb of molecular data were obtained (Table 1). Combined with optical mapping data, we finally yielded a *P. haitanensis* genome with a size of 53.3 Mb. Among the 195 scaffolds, 11 pseudomolecules had lengths larger

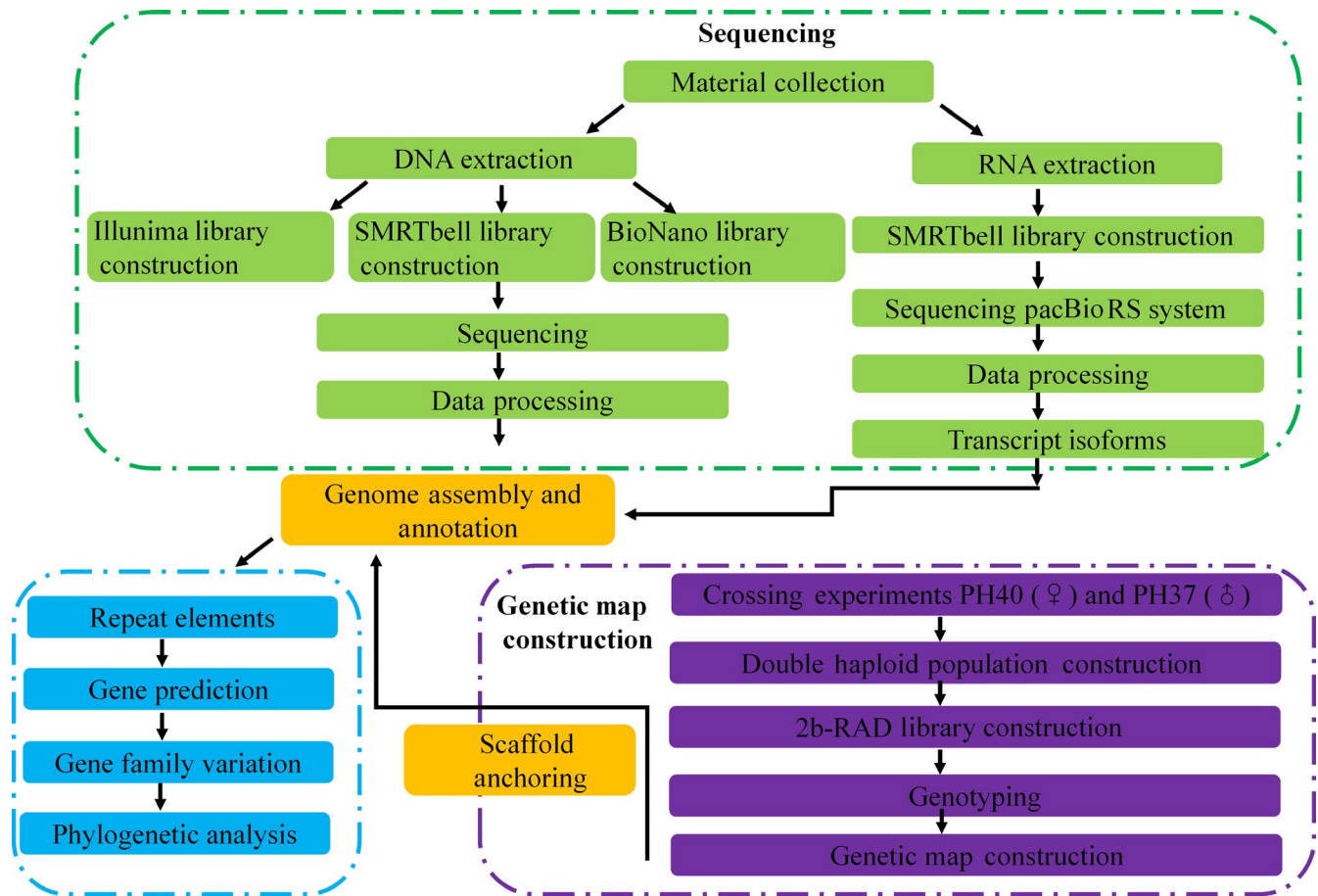


**FIGURE 1** A workflow for the genome sequencing and genetic map construction [Colour figure can be viewed at [wileyonlinelibrary.com](http://wileyonlinelibrary.com)]

	Sequencing platforms	Library size	Data size (Gb)	Depth
DNA library	Illumina	500 bp	22.1	220
	Illumina	5 kb	1.8	47
	PacBio	20 kb	6.4	99
	BioNano	~	93	1,860
RNA library	PacBio	1–2 kb	1.5	12
		2–3 kb	1.3	12
		>3 kb	1.5	12

**TABLE 1** Genome and transcriptome sequencing information of *Pyropia haitanensis*

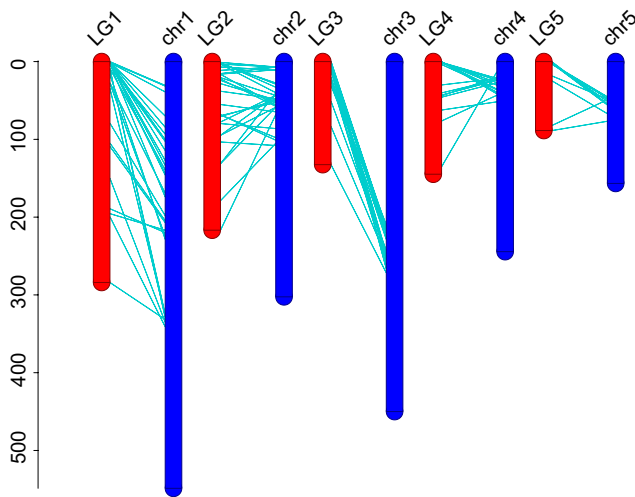
than 0.4 Mb and covered 88.4% of the genome region. The contig N50 and scaffold N50 were 510.3 kb and 5.8 Mb, respectively, and the length of the longest scaffold was 7.6 Mb (Table 2). The average GC content of this genome was as high as 67.9%, which is the highest among all the published algal genomes. The phenomenon of high GC content was also found in the Bangiophyceae species *Po. umbilicalis* (65.8%) (Brawley et al., 2017) and green algae *Chlamydomonas reinhardtii* (64%) (Merchant et al. 2007). Compared with the assembly results of the published macroalgae, including *Chondrus crispus* (scaffold N50 = 240.0 kb), *Po. umbilicalis* (scaffold N50 = 202.0 kb) and *Saccharina japonica* (scaffold N50 = 252.0 kb), the assembly of *P. haitanensis* genome had the fewest scaffolds and the longest N50 and the highest contiguity and coverage (Ye et al., 2015).

### 3.2 | Anchor scaffolds by genetic maps

The genome sequencing of male and female parents and their offspring produced 32,327,297, 35,177,866 and 1,031,682,186 reads, respectively. These reads then were mapped to the genome for subsequent genotyping. The results showed that 1,367 SNPs were shared between the two parents. One hundred and twenty-nine loci that met the linkage requirement were used to construct the genetic map. Finally, five linkage groups were constructed using these markers, with a number of markers ranging from 9 to 45. The length per group ranged from 88.6 cM to 284.0 cM, with an average of 171.4 cM. Based on the markers and genetic distance, 10 pseudomolecules representing 80.9% of the total assembly (42.7 Mb)

**TABLE 2** Statistics of the final assembly of *Pyropia haitanensis* genome

	Contig	Scaffold	BioNano
Total sequences	1,497	230	195
Total bases	57,754,774	50,812,391	53,254,677
Min sequence length	504	740	60
Max sequence length	2,019,106	3,335,433	7,561,339
Average sequence length	38,580.3	220,923.4	273,100.9
N50 length	538,396	1,023,154	5,758,810
N90 length	14,603	143,036	158,429
(G + C)s	69.9%	71.2%	67.8%

**FIGURE 2** Anchor scaffolds from *Pyropia haitanensis* according to genetic maps. The red bar presents the linkage groups generated from genetic maps. The blue bar presents the chromosomes generated via genome assembly [Colour figure can be viewed at [wileyonlinelibrary.com](http://wileyonlinelibrary.com)]

were anchored and orientated to the 5 linkage groups (Figure 2). Among them, pseudomolecules 12, 26, 32 and 110 were anchored to one chromosome, and pseudomolecule 9 was mapped to one chromosome. Meanwhile, pseudomolecules 13 and 27 and pseudomolecules 80 and 201 were placed on two different chromosomes, respectively, based on the markers and their distance. The remaining pseudomolecule 140 was anchored to one chromosome. The number of linkage groups established in this study is consistent with the cytological observations (Tseng & Sun, 1989; Yan et al., 2008).

### 3.3 | Genome evaluation

To assess the quality of the assembled genome, three approaches were used. First, the final assembled genome size of this species (53.3 Mb) was similar to the size calculated based on the K-mer frequency distribution (46.5 Mb). Second, we obtained a total of 17,383 unigenes from the PacBio system. Then, these transcriptome sequencing data were mapped to the current assembly by BLAT (Kent, 2002), and >87.2% of PacBio isoforms could be successfully aligned. Third, we performed Benchmarking Universal Single-Copy Orthologs (BUSCO) analysis, and 85.5% of the eukaryotic single-copy genes were detected in the *P. haitanensis* genome. This number is higher than the values in *C. crispus* (84.5%) and *Po. umbilicalis* (74.3%) (Figure S3). Interestingly, we also noticed that the 'complete' percentage of BUSCO in red algae was generally lower than those in other species. The reason for this possibly lies in independent evolution after primary endosymbiosis, leading to great genome diversity in red algae (e.g. reduction of the genome contents of the red algae (Qiu, Price, Yang, Yoon, & Bhattacharya, 2015)). The relative lack of red algal genome information in public databases might be another reason.

### 3.4 | Repeat elements

For the repeat element analysis, the results showed that the repeat elements identified in *P. haitanensis* constituted 24.2% of the whole genome, including 14.6% as tandem repeat sequences and 9.6% as interspersed repeats. Among the tandem repeats, a total of 26,822

**TABLE 3** Composition of repeat elements in genome of *Pyropia haitanensis*

Class	Order	Superfamily	Number	Length (bp)	Percentage (%)
Interspersed repeats	LTR	Gypsy	413	1,327,093	2.49
		Copia	544	278,151	0.52
		Caulimovirus	83	114,994	0.22
		Other LTR	76	85,379	0.16
	DNA	CMC-EnSpm	83	80,307	0.15
		PIF-Harbinger	331	253,169	0.48
		PiggyBac	228	69,767	0.13
Unknown			10,009	2,874,529	5.40
Tandem repeats	Microsatellite		26,822	1,695,878	3.18
	Minisatellite		60,360	4,290,390	8.06
	Satellite		3,586	1,776,700	3.34

microsatellites were identified, accounting for 3.2% of the genome. In addition, 60,360 (8.1%) minisatellite and 3,586 (3.3%) satellite DNAs were identified. LTR elements represented the majority of

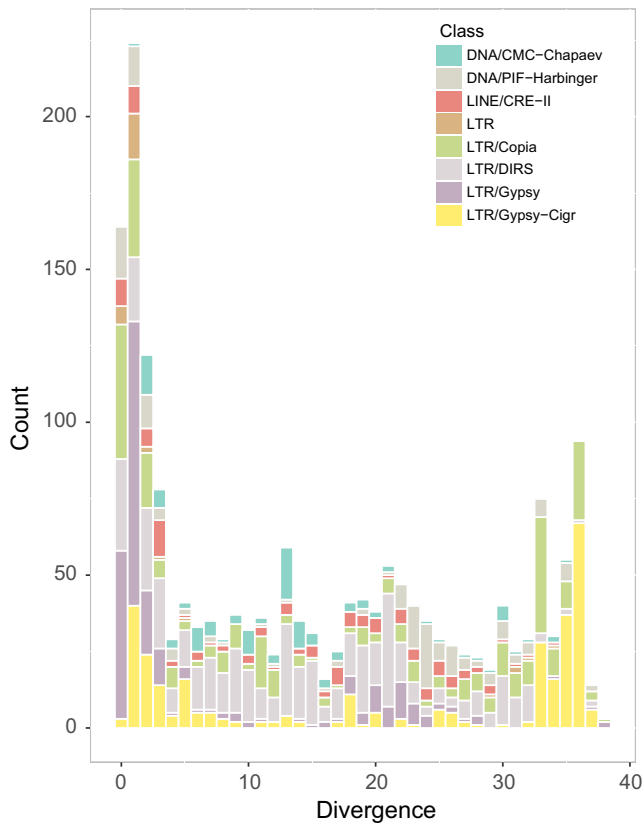


**FIGURE 3** A repeat landscape of the *Pyropia haitanensis* genome showing the expansion and decline of transposable elements [Colour figure can be viewed at [wileyonlinelibrary.com](http://wileyonlinelibrary.com)]

the confirmed interspersed repeats, occupying 3.4% of the genome, while the DNA elements comprised 0.8% (Table 3, Figure 3). Among LTRs, 1,040 full-length LTRs were predicted, 544 of which belonged to the Copia superfamily, 413 belonged to the Gypsy superfamily and 83 belonged to Caulimovirus superfamily. The remaining 76 LTRs were not full length and occupied 0.2% of the genome. When compared with closely related species, we noticed that the *Po. umbilicalis* genome had a substantial repeat element (43.9%) in its 87.7 Mb genome, including 17.7% DNA transposons (15.5 Mb) and 17.0% LTR elements (14.9 Mb) (Brawley et al., 2017). Comparison of the repeat landscape of the *P. haitanensis* genome and those in other species in red algae (Price et al., 2019) showed that the LTRs can be attributed to genome size variation.

### 3.5 | Gene prediction

After repeats' masking, de novo prediction predicted 11,725 gene models for *P. haitanensis*. Based on the homologous protein database established from the five red algae mentioned above, 31,389 protein-coding sequences were obtained. At the same time, we predicted 11,871 gene models using PASA software. Finally, EVM was used to integrate these gene models from the above methods to obtain a gene data set with 10,930 protein-coding sequences (ORFs), which is comparable to the gene repertoire of other sequenced red algae genomes (Bhattacharya et al., 2013; Brawley et al., 2017; Collén et al., 2013; Lee et al., 2018; Nozaki et al., 2007). These protein-coding genes in *P. haitanensis* were further employed to analyse their functions using several public databases. We identified 7,356 and 10,374 genes that showed homology to proteins in the NR and InterPro databases, respectively (Figure S4). A total of 3,147 genes were assigned to GO

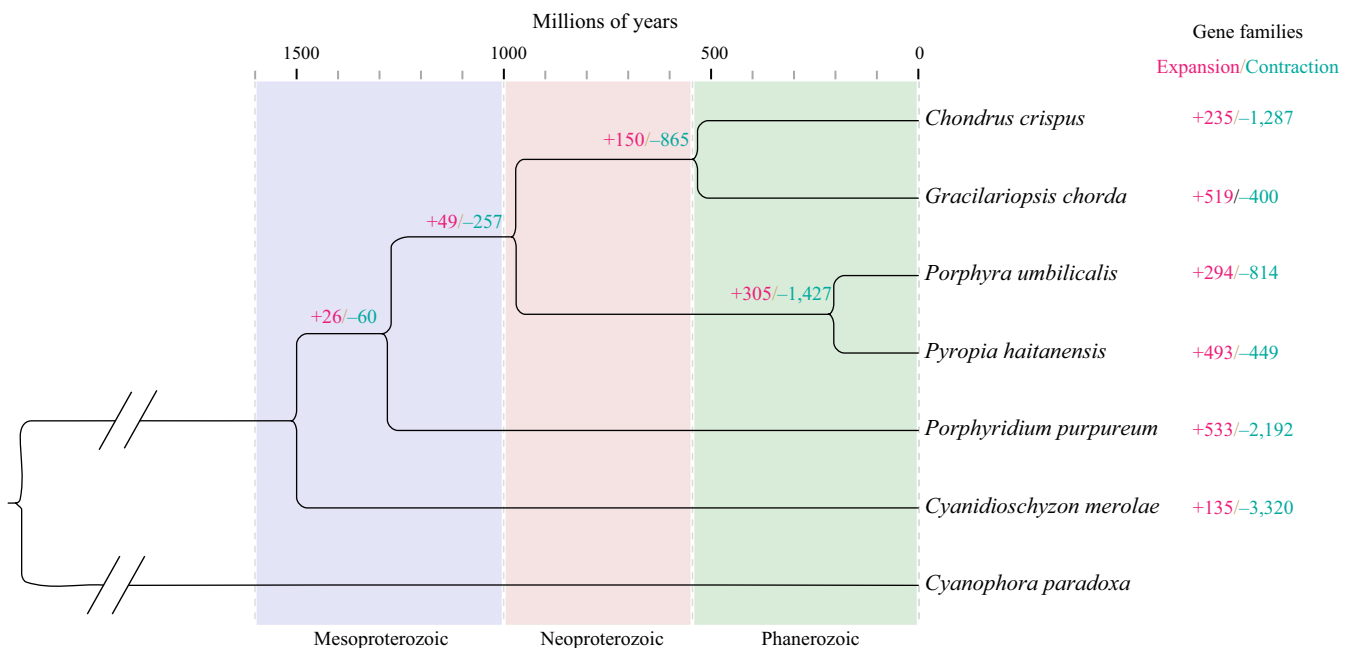


**FIGURE 4** Phylogenetic analyses to reveal the evolutionary relationship and gene families and expansion in red algae. Six hundred and twenty-two single-copy orthologous genes within *Pyropia haitanensis* and six other species were used in phylogenetic analyses [Colour figure can be viewed at [wileyonlinelibrary.com](http://wileyonlinelibrary.com)]

**TABLE 4** ROS-ABA signalling pathway-related genes in *Pyropia haitanensis* and other red algae

Gene name	Gene function	<i>P. haitanensis</i>	<i>Porphyra umbilicalis</i>	<i>Chondrus crispus</i>	<i>Porphyridium purpureum</i>	<i>Cyanidioschyzon merolae</i>
ROS production						
RBOH	NADPH oxidase	ph10359.t1	OSX70888.1	ccriXP_005718545.1	ppur evm.model.contig_2134.3	Cm XP_005535894.1
		ph07364.t1	OSX75422.1	ccriXP_005719187.1	ppur evm.model.contig_2149.17	Cm XP_005538587.1
		ph06070.t1	OSX74398.1	ccriXP_005718335.1	ppur evm.model.contig_2146.22	
		ph07507.t1	OSX73467.1	ccriXP_005716000.1	ppur evm.model.contig_3670.1	
		ph08568.t1	OSX75676.1		ppur evm.model.contig_502.2	
		ph05196.t1	OSX69054.1			
		ph03740.t1	OSX69091.1			
		ph11172.t1	OSX72018.1			
		ph06827.t1				
		ph03938.t1				
AOX	in mitochondria	ph03278.t1	OSX69369.1	ccriXP_005719100.1	ppur evm.model.contig_2288.11	Cm XP_005536259.1
PTX	in plastid	ph07793.t1	OSX69826.1	ccriXP_005712075.1	ppur evm.model.contig_4450.5	Cm XP_005536398.1
ABA regulatory net						
PYR1/PYL/PCAR	N	N	N	N	N	N
PP2C	type-2C protein phosphatase	ph10951.t1	OSX76330.1	ccriXP_005719405.1	ppur evm.model.contig_3479.1	Cm XP_005536535.1
		ph09239.t1	OSX79480.1	ccriXP_005711405.1	ppur evm.model.contig_510.16	Cm XP_005538832.1
		ph02078.t1	OSX71532.1	ccriXP_005719125.1	ppur evm.model.contig_3807.1	Cm XP_005535984.1
		ph11536.t1	OSX77048.1	ccriXP_005712925.1	ppur evm.model.contig_4456.15	Cm XP_005535913.1
		ph07863.t1	OSX81030.1	ccriXP_005711323.1	ppur evm.model.contig_2501.2	
		ph10321.t1	OSX77620.1		ppur evm.model.contig_3441.20	
		ph02405.t1	OSX69983.1		ppur evm.model.contig_441.27	
		ph06642.t1	OSX71152.1		ppur evm.model.contig_3468.6	
		ph08933.t1			ppur evm.model.contig_528.2	
					ppur evm.model.contig_2082.9	
			ppur evm.model.contig_3620.3			
			ppur evm.model.contig_4590.3			
OST1	Protein OPEN STOMATA kinase	ph00419.t1	OSX79527.1	ccriXP_005711343.1	ppur evm.model.contig_2031.6	
		ph03789.t2	OSX79650.1	ccriXP_005713325.1		
				ccriXP_005716962.1		
				ccriXP_005718769.1		

(Continues)



TABLE 4 (Continued)

Gene name	Gene function	<i>P. haitanensis</i>	<i>Porphyra umbilicalis</i>	<i>Chondrus crispus</i>	<i>Porphyridium purpureum</i>	<i>Cyanidioschyzon merolae</i>
SLAC1	slow anion channel-associated	ph09254.t1	OSX76312.1	ccri XP_005718439.1		ppur evm.model.contig_498.15
G protein-coupled receptor (GPCR)		ph09960.t1	OSX76732.1	ccri XP_005716830.1	ppur evm.model.contig_4450.2	Cm XP_005539542.1
		ph00460.t1	OSX76731.1	ccri XP_005711645.1	ppur evm.model.contig_522.10	Cm XP_005537601.1
		ph10367.t1	OSX70306.1	ccri XP_005711658.1	ppur evm.model.contig_431.16	Cm XP_005535191.1
			OSX68793.1			

classifications. Based on KEGG analysis, we could annotate a total of 1,830 genes (Table S2) and a total of 317 KEGG metabolic pathways in the genome of *P. haitanensis* (Figure S5). Moreover, the CAZyme database annotation showed that a total of 303 genes in the *P. haitanensis* genome were associated with carbohydrate metabolism-related enzymes (Table S3). In addition, 7,041 genes in *P. haitanensis* were assigned to CDD 1,295 superfamilies (Table S4).

### 3.6 | Gene family expansion and contraction

To estimate the gene family expansion and contraction, the genome of *P. haitanensis* combined with five available red algae and an out-group species was selected to define the orthologous genes. We identified 622 single-copy orthologous genes within *P. haitanensis* and the other six species, which were used in phylogenetic analyses in the following study. Analysis suggested the divergence time of *P. haitanensis* and *Po. umbilicalis* was 204.4 Ma (95% highest posterior density (HPD)=164.6–249.7 Ma), indicating that *P. haitanensis* was a more recently diverged lineage in the red algae (Figure 4).

A total of 493 orthologous groups (containing 2,514 genes) harboured more *P. haitanensis* paralogs than *Po. umbilicalis* and were therefore defined as the expanded gene families. They mainly encoded ATP hydrolysis, nucleic acid metabolism, purine metabolism, cytoskeleton-associated proteins, ion-transporting proteins as well as E3 ubiquitin ligase, etc., according to their Pfam annotation (Tables S5 and S6). Meanwhile, 294 groups (containing 1,218 genes) with fewer *P. haitanensis* paralogs were defined as contracted gene families. These encoded phytochelatin synthase, sucrose transporter, cytochrome c oxidase copper chaperone, etc. Although the two closely related species are similar in morphology and physiology, the existence of large amounts of expanded and contracted gene families among them suggests that different environmental pressures have shaped their specific genetic contents to adapt to their individual habitats since they diverged from each other.

### 3.7 | ROS-ABA signalling pathway-related genes in *P. haitanensis*

ROS is an important secondary messenger that is poised at the core of signalling pathway in plants maintaining the normal metabolic fluxes and different cellular functions and responding to environment stresses (Quigley et al., 2009). The production of ROS in cell originated from NADPH oxidases (NOX) located different organelles (cell wall, chloroplast and mitochondria) (Bedard & Krause, 2007). The NOX in cell wall is also considered as ROS-generating respiratory burst oxidase (RBOH). In higher plants, RBOH is a family with more than ten members (Suzuki et al., 2011). We identified 10 members of RBOH in *P. haitanensis*, 8 in *P. umbilicalis*, 4 in *C. crispus* and 2 in *Cyanidioschyzon merolae* (Table 4). Compared to single-cell red algae, RBOH in *P. haitanensis* endured significant expanding during evolution. The numbers of AOX and PTX in *P. haitanensis* are 2, with no significant difference with other red algae species. Under the downstream signal pathway activated by ROS, MAPK cascade

is highly conserved and can be activated by phosphorylation (Xing, Ginty, & Greenberg, 1996). It plays major role in signal transduction of diverse stress responses even in combination of many stresses. The activation of MAPK cascade firstly is inhibited by MAPK repressor while induced by ROS (Son et al., 2011). The dual-specificity protein tyrosine phosphatase (DSPTP) is MAPK repressor in ROS pathway (Martell, Angelotti, & Ullrich, 1998). Only 1 was identified, *P. haitanensis*; however, 8 and 5 was identified in single-cell red algae species, *P. purpureum* and *C. merolae*, respectively. When the MAPK cascade was activated, the phosphorylation event can further activated many downstream factors, including transcript factors (TFs) etc. At present, MYB44, HSFA and ERF factors were identified to be activated by MAPK and involved in many stress and development process. We identified 16 MYB family TFs in *P. haitanensis*, including 12 MYB-like, respectively. Yet, only 1 HSFA was identified in *P. haitanensis*. There are no significant differences in the numbers of these two-type TFs in all red algae species studied. It was noting that ERF factor did not exist in either specie, which is an important TFs in ethylene signalling pathway.

ABA signalling pathway plays important in response to environmental stress, especially drought stress (Davies, Kudoyarova, & Hartung, 2005). The turning on of this pathway is dependent on the ABA receptor binding to ABA. Currently, the ABA receptor widely studied including PYR1/PYL/PCAR component. Its binding to ABA can inhibit PP2C, further inhibit OST1 kinase and activate MAPK. After that, the downstream response factors were activated. In addition, OST1 can activate the slow anion channel-associated (SLAC). We did not identify the presence of PYR1/PYL/PCAR type receptor in either red algae, but identified G protein receptor (GPCR), which is another receptor binding to ABA. The number of GPCR in *P. haitanensis* is 3. There are 10 PP2C in *P. haitanensis*, yet only 5 in *P. umbilicalis*, which indicated this gene family endured expanding in *P. haitanensis*. OST1 (1) and SLAC (2) were also identified in different red algae with no significant difference in numbers. Numerous reports highlight the importance of the ROS-ABA signalling pathway in responding to drought stress in higher plants (Cruz de Carvalho, 2008; Gollack, Li, Mohan, & Probst, 2014). These stress factors in the intertidal zones make *Pyropia* highly environmentally tolerant for different stress, including osmotic stress, temperature stress and light stress (Hwang, Chung, & Oh, 1997). Therefore, we speculated that the expanded genes in ROS-ABA signalling pathway were closely related to the ability of environmental adaptation in *P. haitanensis*.

## 4 | CONCLUSIONS

In this study, we reported a high-quality nuclear genome of *Pyropia haitanensis*, a red algal species of great economic, ecological and research value. We adopted multiple sequencing techniques to achieve an assembly with high contiguity and coverage. The investigation of genome characteristics and functional features yields further insights regarding the phylogenetic diversity of *P. haitanensis*. This genome will not only be a fundamental resource for

deciphering the molecular mechanisms underlying the developmental processes of *P. haitanensis* and environmental adaptation mechanisms of intertidal seaweeds, but also help to reconstruct the evolutionary history of red algae.

## AUTHOR CONTRIBUTIONS

Y.X.M. and D.M.W. conceived the study. C.M., X.Z.Y. and P.P.S. performed the experiments. K.P.X., G.Q.B., Y.L., F.N.K., X.H.T., Y.G. and G.Y.D. analysed and interpreted the assembly and annotations. K.P.X. and G.Q.B. performed the comparative genome analysis. C.M. and K.P.X. wrote the manuscript with input from all authors.

## ORCID

Min Cao  <https://orcid.org/0000-0002-8479-5159>

## DATA AVAILABILITY STATEMENT

The DNA sequencing data have been deposited into the NCBI Sequence Read Archive under the BioProject: PRJNA503796.

## REFERENCES

- Abascal, F., Zardoya, R., & Posada, D. (2005). ProtTest: Selection of best-fit models of protein evolution. *Bioinformatics*, 21 (9): 2104–2105.
- Archibald, J. M. (2012). The evolution of algae by secondary and tertiary endosymbiosis. *Advances in botanical research* 64, 87–118.
- Ari, Ş., & Arikan, M. (2016). Next-generation sequencing: Advantages, disadvantages, and future. In K. R. Hakeem, H. Tombuloğlu, & G. Tombuloğlu (Eds). *Plant omics: Trends and applications* (pp. 109–135). Cham: Springer.
- Bedard, K., & Krause, K. H. (2007). The NOX family of ROS-generating NADPH oxidases: Physiology and pathophysiology. *Physiological Reviews*, 87(1), 245–313. <https://doi.org/10.1152/physrev.00044.2005>
- Bengtson, S., Sallstedt, T., Belivanova, V., & Whitehouse, M. (2017). Three-dimensional preservation of cellular and subcellular structures suggests 1.6 billion-year-old crown-group red algae. *PLoS Biology*, 15(3), e2000735.
- Benson, G. (1999). Tandem repeats finder: A program to analyze DNA sequences. *Nucleic Acids Research*, 27(2), 573–580. <https://doi.org/10.1093/nar/27.2.573>
- Bhattacharya, D., Price, D. C., Chan, C. X., Qiu, H., Rose, N., Ball, S., ... Yoon, H. S. (2013). Genome of the red alga *Porphyridium purpureum*. *Nature Communications*, 4, 1941. <https://doi.org/10.1038/ncomm.s2931>
- Biscotti, M. A., Olmo, E., & Heslop-Harrison, J. P. (2015). Repetitive DNA in eukaryotic genomes.
- Blouin, N. A., Brodie, J. A., Grossman, A. C., Xu, P., & Brawley, S. H. (2011). *Porphyra*: A marine crop shaped by stress. *Trends in Plant Science*, 16(1), 29–37. <https://doi.org/10.1016/j.tplants.2010.10.004>
- Boetzer, M., Henkel, C. V., Jansen, H. J., Butler, D., & Pirovano, W. (2010). Scaffolding pre-assembled contigs using SSPACE. *Bioinformatics*, 27(4), 578–579. <https://doi.org/10.1093/bioinformatics/btq683>
- Brawley, S. H., Blouin, N. A., Ficko-Blean, E., Wheeler, G. L., Lohr, M., Goodson, H. V., & Marriage, T. N. (2017). Insights into the red algae and eukaryotic evolution from the genome of *Porphyra umbilicalis*

- (Bangiophyceae, Rhodophyta). *Proceedings of the National Academy of Sciences*, 114(31), E6361–E6370.
- Capella-Gutiérrez, S., Silla-Martínez, J. M., & Gabaldón, T. (2009). trimAl: a tool for automated alignment trimming in large scale phylogenetic analyses. *Bioinformatics*, 25 (15): 1972–1973.
- Chen, N. (2004). Using repeat masker to identify repetitive elements in genomic sequences. *Current Protocols in Bioinformatics*, 5(1), 4–10.
- Chin, C.-S., Alexander, D. H., Marks, P., Klammer, A. A., Drake, J., Heiner, C., ... Korlach, J. (2013). Nonhybrid, finished microbial genome assemblies from long-read SMRT sequencing data. *Nature Methods*, 10(6), 563. <https://doi.org/10.1038/nmeth.2474>
- Collen, J., Porcel, B., Carre, W., Ball, S. G., Chaparro, C., Tonon, T., ... Boyen, C. (2013). Genome structure and metabolic features in the red seaweed *Chondrus crispus* shed light on evolution of the Archaeplastida. *Proceedings of the National Academy of Sciences of the United States of America*, 110(13), 5247–5252. <https://doi.org/10.1073/pnas.1221259110>
- Cruz de Carvalho, M. H. (2008). Drought stress and reactive oxygen species: Production, scavenging and signaling. *Plant Signaling & Behavior*, 3(3), 156–165. <https://doi.org/10.4161/psb.3.3.5536>
- Davies, W. J., Kudoyarova, G., & Hartung, W. (2005). Long-distance ABA signaling and its relation to other signaling pathways in the detection of soil drying and the mediation of the plant's response to drought. *Journal of Plant Growth Regulation*, 24(4), 285. <https://doi.org/10.1007/s00344-005-0103-1>
- Drummond, A. J., Suchard, M. A., Xie, D., & Rambaut, A. (2012). Bayesian phylogenetics with BEAUti and the BEAST 1.7. *Molecular Biology and Evolution*, 29(8), 1969–1973.
- English, A. C., Richards, S., Han, Y. I., Wang, M., Vee, V., Qu, J., ... Gibbs, R. A. (2012). Mind the gap: Upgrading genomes with Pacific Biosciences RS long-read sequencing technology. *PLoS ONE*, 7(11), e47768. <https://doi.org/10.1371/journal.pone.0047768>
- Fu, X., Dou, J., Mao, J., Su, H., Jiao, W., Zhang, L., ... Bao, Z. (2013). RADtyping: An integrated package for accurate de novo co-dominant and dominant RAD genotyping in mapping populations. *PLoS ONE*, 8(11), e79960. <https://doi.org/10.1371/journal.pone.0079960>
- Golldack, D., Li, C., Mohan, H., & Probst, N. (2014). Tolerance to drought and salt stress in plants: Unraveling the signaling networks. *Frontiers in Plant Science*, 5, 151. <https://doi.org/10.3389/fpls.2014.00151>
- Guo, Y., Gu, X., Jiang, Y., Zhu, W., Yao, L., Liu, Z., ... Wang, L. (2018). Antagonistic effect of laver, *Pyropia yezonensis* and *P. haitanensis*, on subchronic lead poisoning in rats. *Biological Trace Element Research*, 181(2), 296–303. <https://doi.org/10.1007/s12011-017-1050-y>
- Haas, B. J., Salzberg, S. L., Zhu, W., Pertea, M., Allen, J. E., Orvis, J., ... Wortman, J. R. (2008). Automated eukaryotic gene structure annotation using EVIDENCEModeler and the program to assemble spliced alignments. *Genome Biology*, 9(1), R7. <https://doi.org/10.1186/gb-2008-9-1-r7>
- Herron, M. D., Hackett, J. D., Aylward, F. O., & Michod, R. E. (2009). Triassic origin and early radiation of multicellular volvocine algae. *Proceedings of the National Academy of Sciences of the United States of America*, 106(9), 3254–3258. <https://doi.org/10.1073/pnas.0811205106>
- Hoek, C., Mann, D., Jahns, H. M., & Jahns, M. (1995). *Algae: An introduction to phycology*. Cambridge, UK: Cambridge University Press.
- Huelsenbeck, J. P., & Ronquist, F. (2001). MRBAYES: Bayesian inference of phylogenetic trees. *Bioinformatics*, 17(8), 754–755. <https://doi.org/10.1093/bioinformatics/17.8.754>
- Hwang, M. S., Chung, I. K., & Oh, Y. S. (1997). Temperature responses of *Porphyra tenera* Kjellman and *P. yezoensis* Ueda (Bangiales, Rhodophyta) from Korea. *Algae*, 12(3), 207–207.
- Katoh, K., Kuma, K. I., Toh, H., & Miyata, T. (2005). MAFFT version 5: Improvement in accuracy of multiple sequence alignment. *Nucleic Acids Research*, 33(2), 511–518.
- Kent, W. J. (2002). BLAT—the BLAST-like alignment tool. *Genome Research*, 12(4), 656–664. <https://doi.org/10.1101/gr.229202>
- Langmead, B., Trapnell, C., Pop, M., & Salzberg, S. L. (2009). Ultrafast and memory-efficient alignment of short DNA sequences to the human genome. *Genome Biology*, 10(3), R25. <https://doi.org/10.1186/gb-2009-10-3-r25>
- Lee, J. M., Yang, E. C., Graf, L., Yang, J. H., Qiu, H., Zelzion, U., ... Yoon, H. S. (2018). Analysis of the draft genome of the red seaweed *Gracilariopsis chorda* provides insights into genome size evolution in Rhodophyta. *Molecular Biology and Evolution*, 35(8), 1869–1886. <https://doi.org/10.1093/molbev/msy081>
- Li, L., Stoeckert, C. J., & Roos, D. S. (2003). OrthoMCL: Identification of ortholog groups for eukaryotic genomes. *Genome Research*, 13(9), 2178–2189. <https://doi.org/10.1101/gr.1224503>
- Luo, R., Liu, B., Xie, Y., Li, Z., Huang, W., Yuan, J., ... Wang, J. (2012). SOAPdenovo2: An empirically improved memory-efficient short-read de novo assembler. *Gigascience*, 1(1), 18. <https://doi.org/10.1186/2047-217X-1-18>
- Martell, K. J., Angelotti, T., & Ullrich, A. (1998). Dual-specificity protein tyrosine phosphatases. *Molecules and Cells*, 8(1), 2–11.
- Merchant, S. S., Prochnik, S. E., Vallon, O., Harris, E. H., Karpowicz, S. J., Witman, G. B., ... Marshall, W. F. (2007). The *Chlamydomonas* genome reveals the evolution of key animal and plant functions. *Science*, 318(5848), 245–250.
- Müller, K. M., Sheath, R. G., Vis, M. L., Crease, T. J., & Cole, K. M. (1998). Biogeography and systematics of *Bangia* (Bangiales, Rhodophyta) based on the Rubisco spacer, rbc L gene and 18S rRNA gene sequences and morphometric analyses. 1. North America. *Phycologia*, 37(3), 195–207.
- Neely, R. K., Deen, J., & Hofkens, J. (2011). Optical mapping of DNA: Single-molecule-based methods for mapping genomes. *Biopolymers*, 95(5), 298–311.
- Nozaki, H., Takano, H., Misumi, O., Terasawa, K., Matsuzaki, M., Maruyama, S., ... Kuroiwa, T. (2007). A 100%-complete sequence reveals unusually simple genomic features in the hot-spring red alga *Cyanidioschyzon merolae*. *BMC Biology*, 5(1), 28. <https://doi.org/10.1186/1741-7007-5-28>
- Price, D. C., Goodenough, U. W., Roth, R., Lee, J.-H., Kariyawasam, T., Mutwil, M., ... Bhattacharya, D. (2019). Analysis of an improved *Cyanophora paradoxa* genome assembly. *DNA Research*, 26(4), 287–299.
- Qiu, H., Price, D. C., Yang, E. C., Yoon, H. S., & Bhattacharya, D. (2015). Evidence of ancient genome reduction in red algae (Rhodophyta). *Journal of Phycology*, 51(4), 624–636. <https://doi.org/10.1111/jpy.12294>
- Quigley, M., Conley, K., Gerkey, B., Faust, J., Foote, T., Leibs, J., Ng, A. Y. (2009). ROS: an open-source Robot Operating System. In ICRA workshop on open source software (Vol. 3, No. 3.2, p. 5).
- Rambaut, A., Drummond, A. J., Xie, D., Baele, G., & Suchard, M. A. (2018). Posterior summarisation in Bayesian phylogenetics using Tracer 1.7. *Systematic Biology*, 67(5), 901–904.
- Reyes-Prieto, A., Weber, A. P., & Bhattacharya, D. (2007). The origin and establishment of the plastid in algae and plants. *Annual Review of Genetics*, 41, 147–168.
- Roberts, R. J., Carneiro, M. O., & Schatz, M. C. (2013). The advantages of SMRT sequencing. *Genome Biology*, 14(6), 405.
- Sahoo, D., Tang, X., & Yarish, C. (2002). *Porphyra*—the economic seaweed as a new experimental system. *Current Science*, 83(11), 1313–1316.
- Smit, A. F., & Hubley, R. (2008). *RepeatModeler Open-1.0*. Retrieved from <http://www.repeatmasker.org>
- Son, Y., Cheong, Y. K., Kim, N. H., Chung, H. T., Kang, D. G., & Pae, H. O. (2011). Mitogen-activated protein kinases and reactive oxygen species: how can ROS activate MAPK pathways?. *Journal of Signal Transduction*, 2011, Article ID 792639, 6.
- Stamatakis, A. (2014). RAXML version 8: a tool for phylogenetic analysis and post-analysis of large phylogenies. *Bioinformatics*, 30(9): 1312–1313.

- Stanke, M., Keller, O., Gunduz, I., Hayes, A., Waack, S., & Morgenstern, B. (2006). AUGUSTUS: Ab initio prediction of alternative transcripts. *Nucleic Acids Research*, 34(suppl\_2), W435–W439.
- Starr, R. C. (1987). UTEX-The culture collection of algae at the University of Texas at Austin. *Journal of Phycology*, 23(3), 1–78.
- Sutherland, J. E., Lindstrom, S. C., Nelson, W. A., Brodie, J., Lynch, M. D., Hwang, M. S., & Farr, T. (2011). A new look at an ancient order: Generic revision of the Bangiales (Rhodophyta) 1. *Journal of Phycology*, 47(5), 1131–1151.
- Suzuki, N., Miller, G., Morales, J., Shulaev, V., Torres, M. A., & Mittler, R. (2011). Respiratory burst oxidases: The engines of ROS signaling. *Current Opinion in Plant Biology*, 14(6), 691–699.
- Tseng, C. K., & Sun, A. (1989). Studies on the alternation of the nuclear phases and chromosome numbers in the life history of some species of *Porphyra* from China. *Botanica Marina*, 32(1), 1–8.
- Van Ooijen, J. (2006). JoinMap@4 Software for the calculation of genetic linkage maps in experimental populations. Kyazma BV, Wageningen, The Netherlands.
- Wang, L., Mao, Y., Kong, F., Cao, M., & Sun, P. (2015). Genome-wide expression profiles of *Pyropia haitanensis* in response to osmotic stress by using deep sequencing technology. *BMC Genomics*, 16(1), 1012. <https://doi.org/10.1186/s12864-015-2226-5>
- Wang, S., Meyer, E., McKay, J. K., & Matz, M. V. (2012). 2b-RAD: A simple and flexible method for genome-wide genotyping. *Nature Methods*, 9(8), 808.
- Wicker, T., Sabot, F., Hua-Van, A., Bennetzen, J. L., Capy, P., Chalhoub, B., ... Schulman, A. H. (2007). A unified classification system for eukaryotic transposable elements. *Nature Reviews Genetics*, 8(12), 973. <https://doi.org/10.1038/nrg2165>
- Xing, J., Ginty, D. D., & Greenberg, M. E. (1996). Coupling of the RAS-MAPK pathway to gene activation by RSK2, a growth factor-regulated CREB kinase. *Science*, 273(5277), 959–963.
- Yan, X. H., He, L. H., Huang, J., Song, W. L., Ma, P., & Aruga, Y. (2008). Cytological studies on *Porphyra haitanensis* Chang et Zheng (Bangiales, Rhodophyta). *Journal of Fisheries of China*, 1, 131–137.
- Yang, E. C., Boo, S. M., Bhattacharya, D., Saunders, G. W., Knoll, A. H., Fredericq, S., ... Yoon, H. S. (2016). Divergence time estimates and the evolution of major lineages in the florideophyte red algae. *Scientific Reports*, 6, 21361.
- Yang, J., Wang, Q., Liu, M. H., & An, L. J. (1999). A simple method for extracting total DNA of seaweeds. *Biotechnol*, 9(4), 39–42.
- Ye, N., Zhang, X., Miao, M., Fan, X., Zheng, Y. I., Xu, D., ... Zhao, F. (2015). Saccharina genomes provide novel insight into kelp biology. *Nature Communications*, 6, 6986. <https://doi.org/10.1038/ncomms7986>
- Yoon, H. S., Müller, K. M., Sheath, R. G., Ott, F. D., & Bhattacharya, D. (2006). Defining the major lineages of red algae (RHODOPHYTA) 1. *Journal of Phycology*, 42(2), 482–492. <https://doi.org/10.1111/j.1529-8817.2006.00210.x>

## SUPPORTING INFORMATION

Additional supporting information may be found online in the Supporting Information section.

**How to cite this article:** Cao M, Xu K, Yu X, et al. A chromosome-level genome assembly of *Pyropia haitanensis* (Bangiales, Rhodophyta). *Mol Ecol Resour*. 2020;20:216–227. <https://doi.org/10.1111/1755-0998.13102>